

Crack initiation at a V-notch—comparison between a brittle fracture criterion and the Dugdale cohesive model

Carole Henninger^{a,*}, Dominique Leguillon^a, Eric Martin^b

^a Institut Jean-Le-Rond-d'Alembert, UMR 7190, université Pierre-et-Marie-Curie, case 162, 4, place Jussieu, 75252 Paris cedex 05, France

^b Laboratoire des composites thermo-structuraux, UMR 5801, université Bordeaux 1, 3, allée de La Boétie, 33600 Pessac, France

Received 18 April 2007; accepted 27 April 2007

Presented by Évariste Sanchez-Palencia

Abstract

The cohesive zone models are an alternative to fracture criteria for the prediction of crack initiation at stress concentration points in brittle materials. We propose here a comparison between the so-called mixed criterion involving a twofold condition (energy and stress) and the Dugdale cohesive model. The predictions of the critical load leading to failure are in perfect agreement and both models conclude that the initial process is unstable except in case of a pre-existing crack. *To cite this article: C. Henninger et al., C. R. Mecanique 335 (2007).*

© 2007 Académie des sciences. Published by Elsevier Masson SAS. All rights reserved.

Résumé

Amorçage d'une fissure en pointe d'entaille en V—comparaison entre un critère de rupture fragile et le modèle de zone cohésive de Dugdale. Les modèles de zone cohésive constituent une alternative aux critères d'amorçage de fissures aux points de concentration de contraintes dans les matériaux fragiles. On se propose ici de comparer le critère dit « mixte », basé sur une double condition en énergie et en contrainte, et le modèle de zone cohésive de Dugdale. Les prédictions de la charge critique d'amorçage coïncident parfaitement, et les deux modèles concluent à l'instabilité du processus d'amorçage sauf dans le cas d'une fissure pré-existante. *Pour citer cet article : C. Henninger et al., C. R. Mecanique 335 (2007).*

© 2007 Académie des sciences. Published by Elsevier Masson SAS. All rights reserved.

Keywords: Rupture; Elasticity; Brittle materials; Cohesive zone

Mots-clés : Rupture ; Élasticité ; Matériaux fragiles ; Zone cohésive

1. Introduction

Within the framework of plane elasticity, the initiation of failure at a V-notch in brittle elastic materials under Mode I loading has been successfully predicted with a mixed criterion based on the critical value of a generalized stress intensity factor (GSIF) [1,2]. Alternatively it can be assumed that a fracture process zone is active in front of

* Corresponding author.

E-mail addresses: henning@lmm.jussieu.fr (C. Henninger), dol@ccr.jussieu.fr (D. Leguillon), martin@lcts.u-bordeaux1.fr (E. Martin).

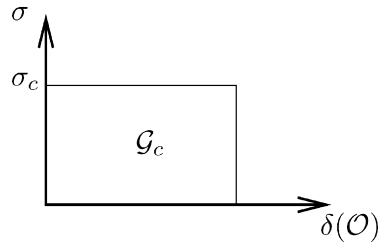


Fig. 1. The Dugdale cohesive model.

Fig. 1. Le modèle de zone cohésive de Dugdale.

the notch tip. The associated cohesive forces can depend on the local opening for a damage model [3–7] or keep constant for a model of perfect plasticity [8]. The latter is chosen to carry on a comparison with the mixed criterion. The constant force is taken equal to the tensile strength σ_c of the material and the crack onset is assumed to occur as:

$$\delta(\mathcal{O}) = \frac{\mathcal{G}_c}{\sigma_c} \tag{1}$$

where $\delta(\mathcal{O})$ is the cohesive zone opening at the notch tip \mathcal{O} and \mathcal{G}_c is the fracture toughness (see Fig. 1). Herein a two-scale analysis using singular elastic fields is carried out and provides the critical GSIF for a set of notch angles. The critical load predictions are compared with those of the mixed criterion [1] and an analysis is made on the stability of the failure mechanism in both models.

2. The cohesive zone model

We consider a V-notched specimen (angle ω , dimensions: $148 \times 90 \times 10$ mm) of PMMA (Young’s modulus: $E = 3250$ MPa, Poisson’s ratio: $\nu = 0.3$, tensile strength: $\sigma_c = 75$ MPa, $\mathcal{G}_c = 0.35$ MPa mm) subjected to a uniaxial tension or displacement (see Fig. 2 left). The crack is expected to grow orthogonally to the direction of sollicitation thus we introduce a cohesive zone of length ℓ in front of the notch tip in that direction. The length ℓ is unknown a priori, what makes the problem non-linear.

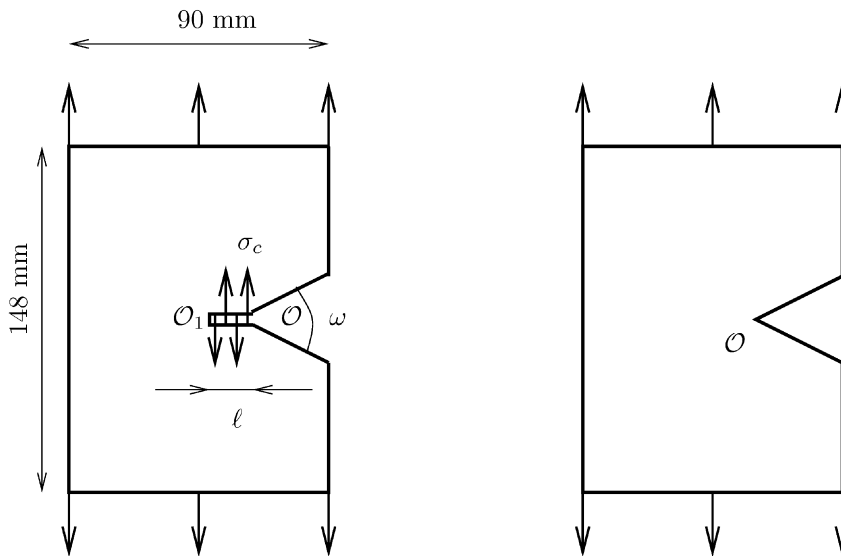


Fig. 2. The actual problem (left) and the ‘outer’ domain (right).

Fig. 2. Le problème réel (gauche) et le domaine « extérieur » (droite).

Table 1

Numerical values of λ , K_I^A , K_I^B and \mathcal{A} (knowledge of \mathcal{A} is unnecessary for $\omega = 180^\circ$)

Tableau 1

Valeurs numériques de λ , K_I^A , K_I^B et \mathcal{A} (la connaissance de \mathcal{A} est inutile pour $\omega = 180^\circ$)

ω ($^\circ$)	0	30	60	90	120	160	180
λ	0.5	0.502	0.512	0.545	0.616	0.819	1
K_I^A (mm $^{-0.5}$)	0.993	0.995	0.987	0.966	0.932	0.851	0.791
K_I^B (mm $^{-0.5}$)	0.6347	0.6354	0.6354	0.6457	0.6696	0.7354	0.7916
\mathcal{A} (MPa $^{-1}$)	5.670	5.648	5.416	4.900	4.040	2.521	

This length ℓ is assumed to be small in regard to the specimen dimensions. Thus the analysis is, in a first step, carried out in an ‘outer’ domain, where the cohesive zone is not visible, i.e. $\ell \rightarrow 0$ (Fig. 2 right). The displacement field in that ‘outer’ domain expands in the vicinity of the notch tip \mathcal{O} as:

$$\underline{U}(x_1, x_2) = \underline{U}(\mathcal{O}) + Kr^\lambda \underline{u}(\varphi) + \dots \quad (2)$$

The constant term $\underline{U}(\mathcal{O})$ is the rigid translation of the origin, (x_1, x_2) and (r, φ) are respectively the Cartesian and polar coordinates with the origin at point \mathcal{O} . The exponent λ is the characteristic exponent of the singularity (smaller the exponent, more critical the singular point) and \underline{u} is the associated displacement mode; they depend on ω and are known analytically or can be computed using a general procedure [9]. As λ ranges between 0.5 and 1 ([10] and Table 1), the associated stress field increases to infinity when approaching \mathcal{O} . The scalar K is the GSIF, it depends on the global geometry and on the loading. The dots correspond to further non-singular terms of the expansion.

Next the analysis is carried out in an ‘inner’ unbounded domain obtained by stretching the actual domain by $1/\ell$ and then considering the limit $\ell \rightarrow 0$. In this inner domain, the cohesive zone has a fixed (unit) length, therefore the non-linearity disappears and the problem splits in two parts \mathcal{P}_A and \mathcal{P}_B .

Matched asymptotics allow writing the solution to \mathcal{P}_A as [1]:

$$\underline{U}^A(x_1, x_2) = \underline{U}(\mathcal{O}) + K\ell^\lambda \underline{V}^A(y_1, y_2) + \dots \quad (3)$$

where (y_1, y_2) are the stretched Cartesian coordinates ($y_i = x_i/\ell$). The displacement field \underline{V}^A fulfils stress-free conditions on the cohesive zone and notch faces and behaves like $\rho^\lambda \underline{u}(\varphi)$ as $\rho \rightarrow \infty$, with $\rho = r/\ell$, as a consequence of matching conditions.

As well, the solution to \mathcal{P}_B can be written:

$$\underline{U}^B(x_1, x_2) = -\sigma_c \ell \underline{V}^B(y_1, y_2) + \dots \quad (4)$$

where \underline{V}^B fulfils a unit tensile condition on the crack faces, stress-free conditions on the notch faces and vanishing remote conditions at infinity.

Eqs. (3) and (4) provide the total displacement field solution to the cohesive zone problem:

$$\underline{U}^\ell(x_1, x_2) = \underline{U}(\mathcal{O}) + K\ell^\lambda \underline{V}^A(y_1, y_2) - \sigma_c \ell \underline{V}^B(y_1, y_2) + \dots \quad (5)$$

The Williams’ expansions of \underline{V}^A and \underline{V}^B in the vicinity of the tip \mathcal{O}_1 are given by:

$$\underline{V}^A(y_1, y_2) = \underline{V}^A(\mathcal{O}_1) + K_I^A \sqrt{\rho} \underline{u}_I(\varphi) + \dots \quad (6)$$

$$\underline{V}^B(y_1, y_2) = \underline{V}^B(\mathcal{O}_1) + K_I^B \sqrt{\rho} \underline{u}_I(\varphi) + \rho \underline{v}(\varphi) + \dots \quad (7)$$

and thus Eqs. (5), (6) and (7) provide:

$$\underline{U}^\ell(x_1, x_2) = \underline{U}(\mathcal{O}) + (K_I^A K\ell^\lambda - K_I^B \sigma_c \ell) \sqrt{\rho} \underline{u}_I(\varphi) - \sigma_c \ell \rho \underline{v}(\varphi) \dots \quad (8)$$

where K_I^A and K_I^B scale the intensity of the singular stress field associated with a crack in an homogeneous material, and \underline{u}_I is the opening mode (since the loading and the geometry are symmetric, the shear mode II vanishes). The non-singular term $\rho \underline{v}(\varphi)$ corresponds to the constant stress conditions on the two faces of the cohesive zone. The fields \underline{V}^A and \underline{V}^B are computed using a finite element method and the GSIF’s K_I^A and K_I^B are extracted using a path-independent integral [9] (see Table 1).

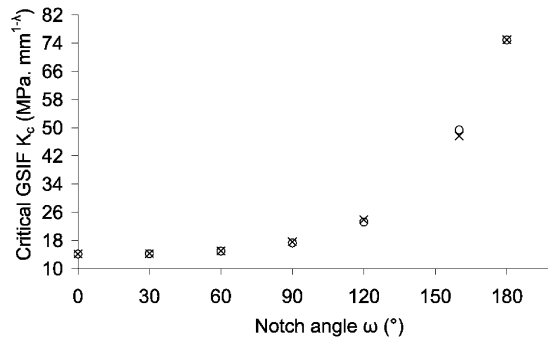


Fig. 3. The critical GSIFs in the cohesive zone model (circles) and in the mixed criterion (cross-shaped markers) versus the notch angle ω .

Fig. 3. Les facteurs d'intensité de contraintes généralisés dans le modèle de zone cohésive (cercles) et dans le critère mixte (croix) en fonction de l'angle d'entaille ω .

3. The crack onset predictions

According to Eq. (5) the opening at the notch tip can be written:

$$\delta(\mathcal{O}) = K \ell^\lambda [V^A](\mathcal{O}) - \sigma_c \ell [V^B](\mathcal{O}) \tag{9}$$

The notation $[V]$ denotes the opening (the normal discontinuity) of \underline{V} .

The cohesive zone is such that the stress field at the tip \mathcal{O}_1 is smooth [3,8]. Using the expansion (8), this condition is:

$$K_I^A K \ell^\lambda - K_I^B \sigma_c \ell = 0 \tag{10}$$

giving an equation for the cohesive zone length ℓ in function of the load (through K), provided the opening $\delta(\mathcal{O})$ does not exceed the critical value \mathcal{G}_c/σ_c (see Eq. (1)).

Combining Eqs. (1), (9) and (10) provides the failure GSIF K_c^z (the critical value of K) for the cohesive zone model:

$$K_c^z = \left(\frac{\mathcal{G}_c}{\bar{\mathcal{A}}} \right)^{1-\lambda} (\sigma_c)^{2\lambda-1} \tag{11}$$

with $\bar{\mathcal{A}} = \left(\frac{K_I^A}{K_I^B} \right)^{\frac{\lambda}{1-\lambda}} [V^A](\mathcal{O}) - \left(\frac{K_I^A}{K_I^B} \right)^{\frac{1}{1-\lambda}} [V^B](\mathcal{O})$.

On the other hand the mixed criterion, based on two necessary conditions in energy and stress [1], provides the following critical value of the GSIF:

$$K_c = \left(\frac{\mathcal{G}_c}{\mathcal{A}} \right)^{1-\lambda} (\sigma_c)^{2\lambda-1} \tag{12}$$

where \mathcal{A} is a geometrical coefficient (dependent on ω), extracted from \underline{V}^A by a path-independent integral [9,1] (see Table 1).

Fig. 3 exhibits K_c^z (circles) and K_c (cross-shaped markers) as a function of the notch angle ω . They are computed using, respectively, Eqs. (11) and (12) (except for $\omega = 180^\circ$). The agreement between both criteria is very good. The maximum deviation is smaller than 4% for $\omega = 160^\circ$. For $\omega = 180^\circ$ the critical GSIF is obtained directly from Eq. (10) ($K_c^z = \sigma_c K_I^B / K_I^A$, noting that, in that case, $K_I^B = K_I^A$), while the mixed criterion provides: $K_c = \sigma_c$. The maximal cohesive zone length (i.e. its length at failure) ranges between 87 μm for $\omega = 0^\circ$ and 224 μm for $\omega = 160^\circ$, what is consistent with the initial assumption of smallness and justifies the asymptotic development.

4. Stability of the initiation process

The brittle fracture criterion leads to the conclusion that, whatever the kind of applied loads, the initial fracture process is brutal for $\omega > 0^\circ$: the crack jumps suddenly to a finite length, [1], while for $\omega = 0^\circ$ the criterion allows

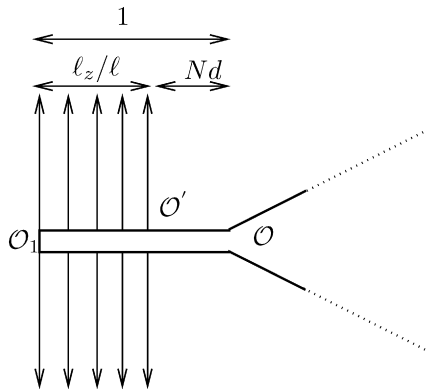
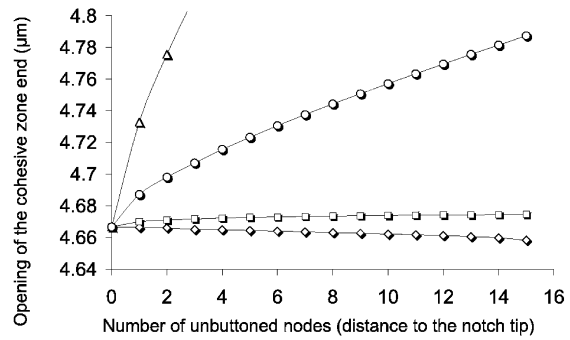


Fig. 4. The modelling of the crack growth.

Fig. 4. Modélisation de la phase d'amorçage.

Fig. 5. The opening of the cohesive zone end for $\omega = 0^\circ$ (diamonds), $\omega = 30^\circ$ (squares), $\omega = 60^\circ$ (circles) and $\omega = 90^\circ$ (triangles) as a function of the distance to the notch tip.Fig. 5. L'ouverture de l'extrémité de la zone cohésive pour $\omega = 0^\circ$ (losanges), $\omega = 30^\circ$ (carrés), $\omega = 60^\circ$ (cercles) et $\omega = 90^\circ$ (triangles) en fonction de la distance à la pointe d'entaille.

infinitesimal crack lengths, as suggested by Griffith. The question is: does the cohesive model, a damage-like model, lead to the same conclusions?

To check that, the crack initiation is simulated by unbuttoning the two nodes at the end of the cohesive zone and by computing the opening $\delta(\mathcal{O}')$ at the end \mathcal{O}' of the new cohesive zone under the constant critical load K_c^z . The process will be unstable if $\delta(\mathcal{O}') > \delta(\mathcal{O})$. Numerically the unbuttoning process consists in splitting the initial cohesive zone of length ℓ (length 1 in the 'inner' domain) into a stress-free cracked zone and a zone where cohesive forces are still acting. Eq. (10) with $K = K_c^z$ and an updated K_I^B provide the actual length ℓ (it is checked that it remains small), and the length of the cohesive zone ℓ_z is given by:

$$\ell_z = \ell(1 - Nd) \quad (13)$$

where N is the number of unbuttoned couples of nodes and d is the mesh size (see Fig. 4).

Fig. 5 exhibits the opening $\delta(\mathcal{O}')$ as a function of the number of unbuttoned couples of nodes N . The crack configuration ($\omega = 0^\circ$) should theoretically exhibit a constant opening, but a slight (note the scale along the vertical axis) pollution is visible due to the fact that for FE computations the remote conditions at infinity are replaced by prescribed conditions at a large (but finite) distance from the origin. In the other configurations ($\omega > 0^\circ$) the crack onset is unstable since the cohesive zone end openings exceed the critical value \mathcal{G}_c/σ_c and then the process of unbuttoning must go on. Note that the number N does not increase to simulate the growth process but to check the independence with respect to the unbuttoned length (mesh independence).

5. Conclusion

A comparison has been carried on between the mixed criterion and the Dugdale cohesive zone model. The agreement between the two models is excellent and both predict an initially unstable crack growth (except for $\omega = 0^\circ$). Further analyses involving cohesive models where forces depend on the opening (Crisfield or Needleman models for instance, [11]) should be very interesting, but it can be reasonably expected that they will lead to similar conclusions.

References

- [1] D. Leguillon, Strength or toughness? A criterion for crack onset at a notch, *Eur. J. Mech. A, Solids* 21 (2002) 61–72.
- [2] Z. Yosibash, A. Bussiba, I. Gilad, Failure criteria for brittle elastic materials, *Int. J. Fract.* 125 (2004) 307–333.
- [3] G.I. Barenblatt, The formation of equilibrium cracks during brittle fracture. General ideas and hypotheses. Axially-symmetric cracks, *J. Appl. Math. Mech.* 23 (3) (1959) 622–636.
- [4] A. Carpinteri, Decrease of apparent tensile and bending strength with specimen size: two different explanations based on fracture mechanics, *Int. J. Solids Struct.* 25 (4) (1989) 407–429.

- [5] A. Needleman, An analysis of tensile decohesion along an interface, *J. Mech. Phys. Solids* 38 (3) (1990) 289–324.
- [6] O. Allix, P. Ladevèze, Interlaminar interface modelling for the prediction of delamination, *Composite Structures* 22 (1992) 235–242.
- [7] G. Alfano, M.A. Crisfield, Finite element interface models for the delamination analysis of laminated composites: mechanical and computational issues, *Int. J. Numer. Methods Engrg.* 50 (2001) 1701–1736.
- [8] D.S. Dugdale, Yielding of steel sheets containing slits, *J. Mech. Phys. Solids* 8 (1960) 100–104.
- [9] D. Leguillon, E. Sanchez-Palencia, *Computation of Singular Solutions in Elliptic Problems and Elasticity*, Masson, Paris, 1987.
- [10] M.L. Williams, Stress singularities resulting from various boundary conditions in angular corners of plates in extension, *J. Appl. Mech.* 19 (1952) 526–528.
- [11] B. Poitou, E. Martin, N. Carrère, D. Leguillon, J.-M. Gatt, Amorçage de fissure au voisinage des interfaces fibre/matrice: comparaison du critère mixte et des modèles de zone cohésive, in: 18^{ème} Congrès Français de Mécanique, Grenoble, 27–31 août 2007.